Shape Coexistence Near Neutron Number $N = 20$: First Identification of the $E0$ Decay from the Deformed First Excited $J^\pi = 0^+$ State in ^{30}Mg

W. Schwerdtfeger,[1] P. G. Thirolf,[1] K. Wimmer,[1] D. Habs,[1] H. Mach,[2] T. R. Rodriguez,[4] V. Bildstein,[3] J. L. Egido,[4] L. M. Fraile,[5] R. Gernhäuser,[3] R. Hertenberger,[1] K. Heyde,[6] P. Hoff,[7] H. Hübel,[8] U. Köster,[9] T. Kröll,[3] R. Krücken,[3] R. Lutter,[1] T. Morgan,[1] and P. Ring[3]

[1]*Ludwig-Maximilians-Universität München, D-85748 Garching, Germany*
[2]*Department of Nuclear and Particle Physics, Uppsala University, SE-75121 Uppsala, Sweden*
[3]*Physik Department E12, Technische Universität München, D-85748 Garching, Germany*
[4]*Departamento de Física Teórica, Universidad Autonoma de Madrid, E-28049 Madrid, Spain*
[5]*Universidad Complutense, E-28040 Madrid, Spain*
[6]*Department of Subatomic and Radiation Physics, Universiteit Gent, B-9000, Gent, Belgium*
[7]*Department of Chemistry, University of Oslo, N-0315 Oslo, Norway*
[8]*Helmholtz-Institut für Strahlen- und Kernphysik, Universität Bonn, D-53115 Bonn, Germany*
[9]*Institut Laue-Langevin, F-38000 Grenoble, France*

(Received 2 August 2008; revised manuscript received 20 February 2009; published 30 June 2009)

The 1789 keV state in ^{30}Mg was identified as the first excited 0^+ state via its electric monopole ($E0$) transition to the ground state. The measured small value of $\rho^2(E0, 0_2^+ \rightarrow 0_1^+) = (26.2 \pm 7.5) \times 10^{-3}$ implies within a two-level model a small mixing of competing configurations with largely different intrinsic quadrupole deformation near the neutron shell closure at $N = 20$. Axially symmetric configuration mixing calculations identify the ground state of ^{30}Mg to be based on neutron configurations below the $N = 20$ shell closure, while the excited 0^+ state mainly consists of two neutrons excited into the $\nu\, 1f_{7/2}$ orbital. The experimental result represents the first case where an $E0$ back decay from a strongly deformed second to the normal deformed first nuclear potential minimum well has been unambiguously identified, thus directly proving shape coexistence at the borderline of the much-debated "island of inversion."

DOI: 10.1103/PhysRevLett.103.012501 PACS numbers: 23.40.−s, 23.20.Js, 23.20.Nx, 27.30.+t

One of the most studied phenomena in the region of neutron-rich atomic nuclei around the $N = 20$ shell closure is the occurrence of strongly deformed ground states in Ne, Na, and Mg isotopes. This so-called "island of inversion" [1] finds its origin in the promotion of a pair of neutrons across the $N = 20$ shell gap, thus leading to the intrusion of deformed low-lying ($2p2h$) configurations below the spherical ($0p0h$) states compared to nuclei closer to β stability. Despite considerable efforts the precise localization of the transition from normal to intruder-dominated configurations is not yet finally settled and even the origin of the large collectivity of the $0^+_{\text{g.s.}} \rightarrow 2^+_1$ transition in ^{32}Mg is still under debate [2]. A coexistence of spherical and deformed 0^+ states is predicted to exist within a small region around $N = 20$ in the neutron-rich Mg nuclei [3,4], the "island of inversion." So far, studies on spectroscopic properties have focused on $B(E2)$ values between the 0^+ ground state and the first excited 2^+ state [5–10]; however, no excited 0^+ state has yet been observed in these nuclei. While ^{32}Mg, which is conventionally considered a closed-shell nucleus, exhibits a strongly deformed ground state as indicated by the large value of $B(E2; 0^+_{\text{g.s.}} \rightarrow 2^+_1) = 454(78)e^2$ fm^4 [5], the ground state of ^{30}Mg is expected to be much less deformed, whereas a (deformed) excited 0^+_2 state is predicted at an energy between 1.7 and 2 MeV [11–14].

It is the purpose of this Letter to report the first identification of the coexisting 0^+_2 state in ^{30}Mg using conversion electron spectroscopy and to discuss the configuration mixing between normal and intruder configurations at the border of the island of inversion. The reported identification of the connecting $E0$ transition between the deformed first excited 0^+ state and the (nearly) spherical ground state represents the first case where an $E0$ back decay from a strongly deformed second potential minimum to the normal deformed first potential well has been unambiguously identified.

Resulting from fast timing γ-spectroscopy studies [15], the 1789 keV level in ^{30}Mg emerged as a strong candidate for the deformed first excited 0^+_2 state due to its long half-life of 3.9(4) ns and the absence of a ground state γ transition. Figure 1 displays the low-energy part of the level scheme of ^{30}Mg [15], triggering our search for the deformed 0^+_2 state in ^{30}Mg via conversion electron spectroscopy following β decay of ^{30}Na at the ISOLDE facility at CERN [16]. In contrast to earlier publications [15], according to new high-statistics experimental data no imbalance between feeding and deexcitation of the 1789 keV level exists any more [17]. The radioactive ^{30}Na atoms [$t_{1/2} = 48.4(17)$ ms] were produced by sending 1.4 GeV protons provided by the CERN PS Booster with an intensity up to 3.2×10^{13} p/pulse onto a UC$_x$/graphite target.

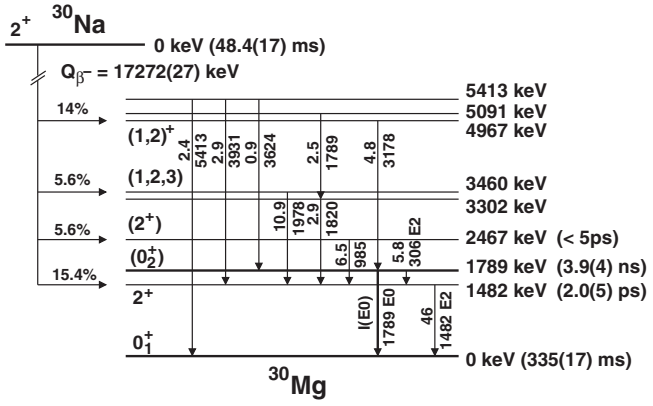

FIG. 1. Low-energy part of the level scheme of ^{30}Mg [15].

On average, every second pulse (average repetition period of 2.4 s) was used. The reaction products diffusing out of the target were surface ionized and the extracted 1^+ ions were mass separated by the ISOLDE High Resolution Separator at a kinetic energy of 40 keV. This $A = 30$ beam was sent to the experimental setup (see Fig. 2). The beam was stopped in the center of the target chamber in a 0.1 mm thick Al foil to examine the β decay of ^{30}Na to excited states of ^{30}Mg. In order to detect the $E0$-decay electrons with high resolution (3.0 keV FWHM) a liquid nitrogen cooled Si(Li) detector (active surface, 500 mm^2; thickness, 5 mm) was used. Its time resolution amounted to ca. 8 ns. The detector was operated in conjunction with a magnetic transport and focusing system consisting of eight wedge-shaped ($Nd_2Fe_{14}B$) permanent magnets ["mini-orange" (MO)] [18]. They create a toroidal magnetic field ($B \sim 160$ mT) arranged around a central Pb absorber (diameter, 16 mm; length, 50 mm) that blocks γ rays from the catcher foil. Towards the catcher foil the absorber was covered by a Cu cap to suppress x-ray production. The transmission efficiency of the spectrometer was 1.8(2)% at 1.788 MeV, optimized for the expected $E0$ transition in ^{30}Mg. A 0.2 mm thick plastic scintillator (BC-404, diameter 50 mm) readout by a 2" photomultiplier tube was

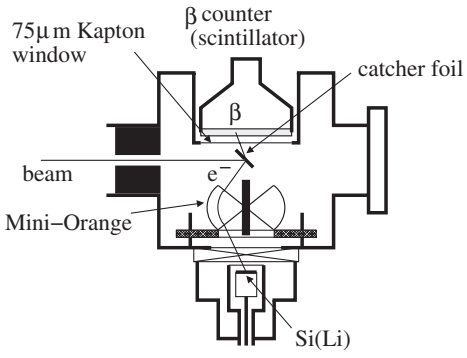

FIG. 2. Sketch of the experimental setup (top view). The germanium detector that was mounted vertically on top of the target chamber is not shown.

mounted at a distance of 13 mm to the target, resulting in a solid angle coverage of $\Omega/4\pi = 21\%$. This detector served as trigger on β-decay electrons and was operated in coincidence with the mini-orange spectrometer above an energy threshold of 300 keV and within a time window of 40 ns. γ rays following β decay were detected using a Ge detector mounted on top of the target chamber and operated with a time resolution of 20 ns above an energy threshold of 60 keV.

In order to achieve optimum sensitivity for the expected weak $E0$ transition, the dominant coincident background from Compton electrons due to the large Q value of the ^{30}Na β decay [17 272(27) keV] was reduced by covering the inside of the Al target chamber by 15 mm thick Teflon plates in order to absorb Compton-scattered electrons. The germanium detector served as monitor of the $A = 30$ beam composition, which turned out to consist almost entirely of ^{30}Na at a total intensity of 4100 decays/s. Since the half-life of ^{30}Na decay is much shorter compared to ^{30}Mg or ^{30}Al originating from the β-decay chain, during the analysis events occurring within a time window of 200 ms after proton impact on the ISOLDE target were selected to enhance the contribution from the short-lived ^{30}Na. The resulting electron spectrum detected with the Si(Li) detector in coincidence with β-decay electrons is shown in Fig. 3. Panel (a) displays the spectrum over a wide energy range, together with the transmission efficiency curve of the MO spectrometer (solid line), that has been derived by a fit through the data points (black circles) obtained from measurements of individual converted transitions using calibrated ^{152}Eu and ^{207}Bi sources. Below the transmission maximum coincident background yield remains from both the β-decay energy spectrum (rapidly increasing with lower β-electron energy) and Compton electrons ($Q_\beta = 17.3$ MeV). In Fig. 3(b) the $0_2^+ \rightarrow 0_1^+$ $E0$ transition at 1788 keV is visible ($E_K = 1.3$ keV). A total of 201(50) (background-corrected) counts were detected in the peak during 143 h in beam time. The monopole strength $\rho^2(E0)$ can be determined by the ratio of $E0$ ($K + L$) conversion intensity to the $E2$ γ intensity and the γ lifetime τ_γ of the 0_2^+ state as [19]

$$\rho^2(E0) = \frac{I_{K+L}(E0)}{I_\gamma(E2)} \frac{1}{\Omega_{K+L}(E0)} \frac{1}{\tau_\gamma}. \quad (1)$$

The γ yield of the $E2$ transition at 306 keV measured with the $\beta - \gamma$ coincidence condition using the Ge detector within a time window of 50 ns is $N_\gamma(E2) = 5.37(4) \times 10^4$, resulting in an efficiency-corrected intensity $I_\gamma = N_\gamma/\epsilon_\gamma = 2.768(20) \times 10^7$ ($\epsilon_\gamma = 0.001\,94$). The half-life of the 0_2^+ state was measured to be 3.9(4) ns [15] [i.e., $\tau_\gamma \approx \tau = 5.6(6)$ ns] and the electronic Ω factor is $\Omega_K = 2.752 \times 10^6$/s [20]. This results in a square of the monopole transition strength $\rho^2(E0) = 26.2(75) \times 10^{-3}$. From the measured intensity ratio $I_{K,L}(E0)/I_\gamma(E2)$ and the known intensity $I_\gamma(E2)$ with respect to β decay of ^{30}Na

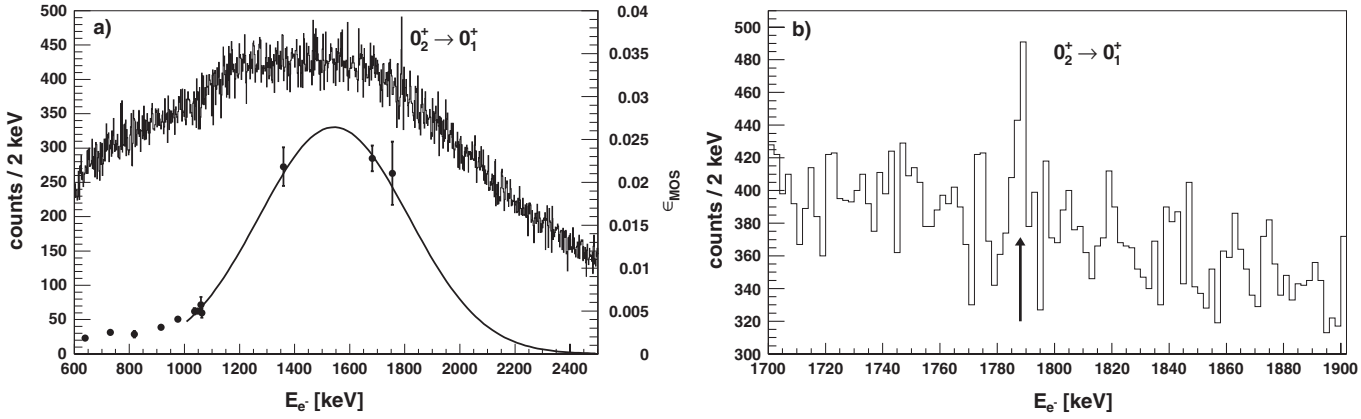

FIG. 3. (a) Background-subtracted electron spectrum measured in coincidence with signals in the plastic detector, gated on time differences ≤ 200 ms between the proton pulse and the β-decay signal. Also shown is the transmission efficiency of the MO spectrometer as derived by a fit through the data points (black circles) obtained from individual converted transitions in calibrated sources (see text). (b) Expanded view to the electron spectrum around the $E0$ transition in ^{30}Mg.

the $E0$ intensity was determined as $I(E0) = 2.0(4) \times 10^{-5}$. The partial $E0$ lifetime (including internal pair creation) was derived as $\tau(E0) = 396(113)$ ns. As will be shown, a small $\rho^2(E0)$ indicates weak coupling between the two potential minima.

In the island of inversion the deformed configuration based on two neutrons being excited from the $\nu\, 1d_{3/2}$ to the intruder orbital $\nu\, 1f_{7/2}$ keeps pace with the normal spherical one as illustrated by the case of ^{32}Mg, where the intruder state even becomes the ground state. In such a situation of competing configurations and in the absence of mixing one expects either a deformed 0_1^+ and a nearly spherical 0_2^+ state or vice versa. Since the $E0$ operator is a *single-particle* one, one expects in both cases small values of the monopole matrix element and hence for the transition strength $\rho^2(E0)$. Inducing configuration mixing, somewhat larger values of $\rho^2(E0)$ can be expected. In ^{30}Mg the small experimental value of $\rho^2(E0) = (26.2 \pm 7.5) \times 10^{-3}$ points towards the presence of small mixing. However, the important question concerning the nature of the two 0^+ states and the amount of mixing of the $\nu\, 1d_{3/2}$ and $\nu\, 1f_{7/2}$ configurations remains to be answered. Concerning the 0_1^+ state there are strong experimental [7,9] and theoretical [11,12,14] indications that in ^{30}Mg the inversion has not taken place.

In order to understand the experimental findings, calculations going beyond the mean field by incorporating configuration mixing [21] have been performed using the finite range density dependent Gogny force with the D1S parametrization [22]. The results of these calculations for ^{30}Mg and ^{32}Mg are listed and compared to experimental values in Table I. The excitation energy of the 0_2^+ state as well as the values for $B(E2; 0_1^+ \rightarrow 2_1^+)$ and $\rho^2(E0)$ agree reasonably well with the experimental values. In Fig. 4(b), the particle number projected (PNP) potential energy curve displays both a mild prolate and an oblate minimum at small deformation and a shoulder at larger β values. Inspecting the neutron single-particle energies in Fig. 4(a), we see that the two minima at moderate deformation correspond to the two minima of the single-particle energies of the $\nu\, 1d_{3/2}$ orbitals just below the Fermi level, while the shoulder appears at deformations at which two neutrons already occupy the $\nu\, 1f_{7/2}$ orbital. The angular momentum projection provides an additional energy lowering with respect to the PNP energy [the full line in 4(b)], and finally configuration mixing leads to the 0_1^+ and 0_2^+ states positioned in the E-β plane [Fig. 4(b)] according to their energy and average deformation. The composition of the collective wave functions of these two states, i.e., the weights of the corresponding β values being admixed,

TABLE I. Results from beyond-mean-field calculations with Gogny force for ^{30}Mg and ^{32}Mg (indicated as "T") compared to experimental values ("E").

		$E_x(2_1^+)$ (MeV)	$E_x(0_2^+)$ (MeV)	$B(E2, 0_1^+ \rightarrow 2_1^+)$ (e^2 fm^4)	$\rho^2(E0) \times 10^{-3}$	$B(E2, 0_2^+ \rightarrow 2_1^+)$ (e^2 fm^4)
^{30}Mg	(T)	2.03	2.11	334.6	46	181.5
	(E)	1.482	1.789	241(31) [9]	26.2 ± 7.5	53(6)
^{32}Mg	(T)	1.35	2.60	455.7	41	56.48
	(E)	0.885	...	454(78) [5]	...	...

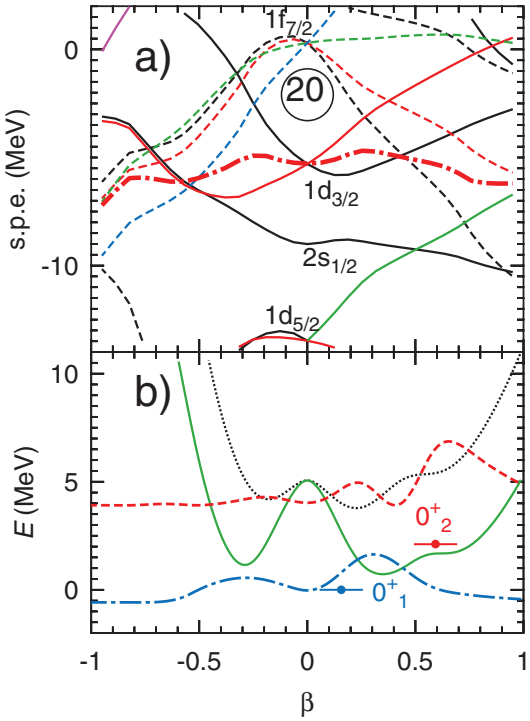

FIG. 4 (color). Theoretical results for ^{30}Mg. (a) Neutron single-particle energies as a function of deformation. The thick dash-dotted line represents the Fermi level. (b) The dotted line corresponds to results of particle number projected (PNP) calculations, the green full line to the $J = 0$ energy surface, and the blue (red) dash-dotted (dashed) line represents the collective wave function of the 0_1^+ (0_2^+) state.

indicates the character of the state. We notice that the 0_1^+ state (blue dot-dashed line) is a mixture of prolate and oblate $\nu\ 1d_{3/2}$ configurations which average to a small intrinsic deformation of $\beta = 0.16$. The 0_2^+ state (blue dashed line), on the other hand, is a well deformed state with $\beta = 0.59$ consisting to a large part of a $\nu\ 1f_{7/2}$ configuration with very small admixtures of the $\nu\ 2d_{3/2}$ configuration. These results are consistent with the experimental finding of a small matrix element connecting both 0^+ levels. It is known [23,24] that the calculation of $\rho^2(E0)$ is very sensitive to small variations of the interaction matrix elements and, in particular, to small admixtures of different shapes. Ideally, one needs to consider triaxial shapes in the calculations. Because of the complexity of a fully triaxial angular momentum projected calculation, at present, we had to restrict to axial symmetric states only.

In order to quantify the mixing amplitude between the deformed and spherical configurations, we have also analyzed our experimental results making use of a phenomenological two-level mixing model [25]. Here $\rho^2(E0)$ strongly depends on the mixing amplitude a between the two intrinsic 0^+ states. Using the deformation values of the two 0^+ states as calculated above [$\beta_1(0_1^+) = 0.16$, $\beta_2(0_2^+) = 0.59$] together with the experimental value of $\rho^2(E0)$, a value of $a^2 = 0.0319(76)$ can be extracted [using Eq. (51) of Ref. [25]], resulting in a value of $a = 0.179(83)$ for the mixing amplitude between the two intrinsic 0^+ states. An identical value of $\beta_2(0_2^+) = 0.59$ can be inferred from the phenomenological Grodzins systematics [26], which empirically correlates the $B(E2; 0_1^+ \rightarrow 2_1^+)$ value and the excitation energy of the first excited 2^+ state (here based on the assignment of the 2467 keV level as being the rotational 2_2^+ state). For ^{30}Mg and ^{32}Mg the $B(E2)$ values predicted by the Grodzins systematics [$256(45)e^2$ fm^4 and $410(73)e^2$ fm^4] agree remarkably well with the experimental values [$241(31)e^2$ fm^4 [9] and $454(78)e^2$ fm^4 [5]]. This also points to rather pure 0^+ and 2^+ states in the two potential minima.

To conclude, conversion electron measurements at ISOLDE have identified the 1789 keV level as the 0_2^+ state in ^{30}Mg. The conversion electrons were measured in coincidence with β-decay electrons using a mini-orange spectrometer. The monopole strength extracted from measuring the $0_2^+ \rightarrow 0_1^+$ $E0$ transition is $\rho^2(E0, {}^{30}\mathrm{Mg}) = (26.2 \pm 7.5) \times 10^{-3}$, corresponding to a partial $E0$ lifetime of $\tau(E0) = 396(113)$ ns. The small value of the monopole strength indicates a weak mixing between shape-coexisting 0^+ states near the "island of inversion." Beyond-mean-field calculations identify the ground state as based on a mixture of prolate and oblate $\nu\ 1d_{3/2}$ orbitals and the excited 0_2^+ state on a rather pure $\nu\ 1f_{7/2}$ level, thereby confirming a sharp borderline of the island of inversion. It would be of great interest to extend this kind of study to a search for the (spherical) 0_2^+ state in ^{32}Mg. However, presently no spectroscopic candidate for this state is available. Because of the much reduced intensity of the ^{32}Na beam, only a low-lying 0_2^+ state could be detected by our technique, while theoretical predictions place this state at around 2 MeV [3,11,12]. Alternatively two-neutron transfer could lead to a population of the 0_2^+ state in ^{32}Mg [27].

This work was supported by BMBF (06ML234, 06MT238, and 06BN109), by the European Commission through I3-EURONS (RIDS-CT-2004-506065), by the Swedish Research Council, by MEC (FPA2007-66069), and by the Spanish Consolider-Ingenio 2010 Program CPAN (CSD2007-00042).

[1] E. K. Warburton, J. A. Becker, and B. A. Brown, Phys. Rev. C **41**, 1147 (1990).
[2] M. Yamagami and N. Van Giai, Phys. Rev. C **69**, 034301 (2004).
[3] K. Heyde and J. L. Wood, J. Phys. G **17**, 135 (1991).
[4] J. L. Wood *et al.*, Phys. Rep. **215**, 101 (1992).
[5] T. Motobayashi *et al.*, Phys. Lett. B **346**, 9 (1995).
[6] H. Iwasaki *et al.*, Phys. Lett. B **522**, 227 (2001).
[7] B. Pritychenko *et al.*, Phys. Lett. B **461**, 322 (1999).
[8] V. Chisté *et al.*, Phys. Lett. B **514**, 233 (2001).

[9] O. Niedermaier *et al.*, Phys. Rev. Lett. **94**, 172501 (2005).
[10] A. Gade *et al.*, Phys. Rev. Lett. **99**, 072502 (2007).
[11] R. Rodríguez-Guzmán, J. L. Egido, and L. M. Robledo, Nucl. Phys. **A709**, 201 (2002).
[12] E. Caurier *et al.*, Nucl. Phys. **A693**, 374 (2001).
[13] F. Nowacki *et al.* (private communicaton); D. Guillemaud-Mueller, Eur. Phys. J. A **13**, 63 (2002).
[14] T. Otsuka, Eur. Phys. J. A **20**, 69 (2003).
[15] H. Mach *et al.*, Eur. Phys. J. A **25**, 105 (2005).
[16] E. Kugler *et al.*, Nucl. Instrum. Methods Phys. Res., Sect. B **70**, 41 (1992).
[17] H. Mach *et al.* (to be published).
[18] J. van Klinken *et al.*, Nucl. Instrum. Methods **130**, 427 (1975).
[19] T. Kibédi and R. H. Spear, At. Data Nucl. Data Tables **89**, 77 (2005).
[20] A. Passoja and T. Salonen, University of Jyväskylä JYFL Report No. RR-2/86, 1986.
[21] T. R. Rodriguez and J. L. Egido, Phys. Rev. Lett. **99**, 062501 (2007).
[22] J. F. Berger, M. Girod, and D. Gogny, Nucl. Phys. **A428**, 23c (1984).
[23] E. Bouchez *et al.*, Phys. Rev. Lett. **90**, 082502 (2003).
[24] A. Petrovici *et al.*, Nucl. Phys. **A665**, 333 (2000).
[25] J. L. Wood *et al.*, Nucl. Phys. **A651**, 323 (1999).
[26] S. Raman, C. W. Nestor, and P. Tikkanen, At. Data Nucl. Data Tables **78**, 1 (2001).
[27] T. Kröll *et al.*, Report No. CERN-INTC-2008-P-239, 2008.